INNOVATIONS JOURNALS

Research Article

Translational Studies Using the MALT1 Inhibitor (*S*)-Mepazine to Induce Treg Fragility and Potentiate Immune Checkpoint Therapy in Cancer

Mauro Di Pilato,[1] Yun Gao,[2] Yi Sun,[3] Amina Fu,[3] Carina Grass,[4] Thomas Seeholzer,[4] Regina Feederle,[5] Irina Mazo,[2,6] Samuel W. Kazer,[2,6] Kevin Litchfield,[7] Ulrich H. von Andrian,[6] Thorsten R. Mempel,[6,8] Russell W. Jenkins,[3,6] Daniel Krappmann,[4] Peter Keller[2]

[1]MD Anderson Cancer Center, University of Texas, Houston, TX, USA
[2]Monopteros Therapeutics, Boston, MA, USA
[3]Massachusetts General Hospital Cancer Center, Harvard Medical School, Boston, MA, USA
[4]Research Unit Signaling and Translation - Signaling and Immunity, Molecular Targets and Therapeutics Center, Helmholtz Munich–German Research Center for Environmental Health, Neuherberg, Germany
[5]Monoclonal Antibody Core Facility, Institute for Diabetes and Obesity, Helmholtz Zentrum München–German Research Center for Environmental Health, Neuherberg, Germany
[6]Harvard Medical School, Boston, MA, USA
[7]Cancer Research UK Lung Cancer Centre of Excellence, University College London Cancer Institute, London, UK
[8]Center for Immunology and Inflammatory Diseases, Massachusetts General Hospital, Boston, MA, USA

Address correspondence to Mauro Di Pilato (mdi@mdanderson.org).

Source of Support: This study received funding from Monopteros Therapeutics, Inc. The funder was involved in study design; collection, analysis, and interpretation of data; and writing of this article and the decision to submit it for publication.

Conflicts of Interest: Mauro Di Pilato, Yun Gao, Irina Mazo, Samuel W. Kazer, and Kevin Litchfield are consultants for Monopteros Therapeutics. Outside of the submitted work, Kevin Litchfield has a patent pending on indel burden and CPI response; he has received speaker fees from Roche tissue diagnostics and research funding from CRUK TDL/Ono/LifeArc alliance and Genesis Therapeutics. Ulrich H. von Andrian and Thorsten R. Mempel are cofounders and shareholders of Monopteros Therapeutics. Russell W. Jenkins has received research support from Monopteros Therapeutics and is on the advisory board for and has a financial interest in XSphera Biosciences; his interests were reviewed and are managed by Massachusetts General Hospital and Partners HealthCare in accordance with their conflict of interest policies. Daniel Krappmann is an advisor to and has received research support from Monopteros Therapeutics. Peter Keller is an employee and shareholder of Monopteros Therapeutics. The remaining authors have no disclosures. The views expressed in this article are those of the authors and not an official position of Monopteros Therapeutics, Inc.

Received: Jul 15, 2022; Revision Received: Nov 17, 2022; Accepted: Dec 12, 2022

Di Pilato M, Gao Y, Sun Y, et al. Translational studies using the MALT1 inhibitor (*S*)-mepazine to induce Treg fragility and potentiate immune checkpoint therapy in cancer. *J Immunother Precis Oncol*. 2023; 6:61–73. DOI: 10.36401/JIPO-22-18.

ABSTRACT

Introduction: Regulatory T cells (Tregs) play a critical role in the maintenance of immune homeostasis but also protect tumors from immune-mediated growth control or rejection and pose a significant barrier to effective immunotherapy. Inhibition of MALT1 paracaspase activity can selectively reprogram immune-suppressive Tregs in the tumor microenvironment to adopt a proinflammatory fragile state, which offers an opportunity to impede tumor growth and enhance the efficacy of immune checkpoint therapy (ICT). **Methods:** We performed preclinical studies with the orally available allosteric MALT1 inhibitor (*S*)-mepazine as a single-agent and in combination with anti-programmed cell death protein 1 (PD-1) ICT to investigate its pharmacokinetic properties and antitumor effects in several murine tumor models as well as patient-derived organotypic tumor spheroids (PDOTS). **Results:** (*S*)-mepazine demonstrated significant antitumor effects and was synergistic with anti-PD-1 therapy in vivo and ex vivo but did not affect circulating Treg frequencies in healthy rats at effective doses. Pharmacokinetic profiling revealed favorable drug accumulation in tumors to concentrations that effectively blocked MALT1 activity, potentially explaining preferential effects on tumor-infiltrating over systemic Tregs. **Conclusions:** The MALT1 inhibitor (*S*)-mepazine showed single-agent anticancer activity and presents a promising opportunity for combination with PD-1 pathway-targeted ICT. Activity in syngeneic tumor models and human PDOTS was likely mediated by induction of tumor-associated Treg fragility. This translational study supports ongoing clinical investigations (ClinicalTrials.gov Identifier: NCT04859777) of MPT-0118, (*S*)-mepazine succinate, in patients with advanced or metastatic treatment-refractory solid tumors.

Keywords: MALT1, cancer immunotherapy, regulatory T cells, fragile Tregs, interferon-γ

INTRODUCTION

$CD4^+$ $FoxP3^+$ regulatory T cells (Tregs) are essential for maintaining self-tolerance and immunological homeostasis.[1,2] They can develop in both the thymus and immune periphery, and T-cell receptor (TCR), costimulatory, and interleukin-2 signals drive their conversion in secondary lymphoid organs from a resting phenotype (central Tregs) to an activated state (effector Tregs). The latter have the ability to traffic to immune effector sites, such as solid tumors. Importantly, although Tregs are generally a stable cell lineage, effector Tregs possess inherent functional plasticity that enables them to adapt to the type of immune response they are regulating.[3]

Although Tregs protect against autoimmune and inflammatory diseases, they also hinder immune-mediated rejection of malignant tumors, and their relatively high frequencies in the tumor microenvironment (TME), especially in proportion to conventional $CD8^+$ T cells, often correlate with poor prognoses for patients with cancer.[4–8] Tumor-associated Tregs use multiple suppressive mechanisms to constrain antitumor immune responses and impede the effectiveness of cancer immunotherapy.[2,6,7,9–13] In particular, although immune checkpoint therapy (ICT) has been transformative in treating a broad range of cancers,[14–16] objective response rates (ORRs) remain low for many cancer types, and initial responders may acquire resistance over time.[12,15, 17,18] Therefore, the use of combination therapies to improve ICT ORRs is an ongoing area of research, and manipulating Tregs is one emergent option.[8,13,15,19,20]

The propensity of suppressive $FoxP3^+$ Tregs to acquire a proinflammatory, "fragile" state under the destabilizing conditions of the TME is an evolving aspect of Treg behavior drawing considerable attention.[2,8,20,21] Studies in murine tumor models have demonstrated such effects using genetic perturbations or pharmacological interventions targeting proteins associated with eTreg function.[22–28] These interventions can "reprogram" tumor-associated Tregs to secrete interferon-γ (IFNγ) and amplify effector lymphocyte infiltration, leading to antitumor benefits. Synergy of such Treg reprogramming with ICT has also been observed in some cases, using either genetic or pharmacological approaches.[24–26,28] Moreover, Treg reprogramming has been reported in patients with cancer on active immunotherapy without signs of autoimmune toxicity.[29] Thus, Treg reprogramming represents a potential opportunity for expanding immunotherapy to unresponsive or poorly responsive cancer types.

Impaired functional behavior of Tregs has also been induced by genetic mutations or pharmacological inhibition of the CARMA1-BCL10-MALT1 (CBM) multiprotein complex. The CBM complex bridges TCR engagement to nuclear factor-κB (NF-κB) and c-Jun N-terminal kinase signaling cascades in T lymphocytes,[30,31] and genetic deficiencies of individual CBM subunits severely impair Treg development and function. For example, genetic deletion of either B cell lymphoma/leukemia 10 (BCL10) or CARD-containing MAGUK protein 1 (CARMA1, also known as caspase-recruitment domain-containing protein 11 [CARD11]) in mature Tregs caused loss of suppressive function, gain of IFNγ expression, and severe autoimmune lymphoproliferative syndromes.[32–34] In contrast, partial reduction of CARMA1 protein through heterozygous CARMA1 deficiency in a mouse melanoma model did not cause systemic inflammatory disease but led to IFNγ secretion by Tregs selectively in the TME and not elsewhere.[34] The resulting antitumor effect was, however, limited by induction of programmed cell death ligand 1 (PD-L1) on tumor cells, causing adaptive immune resistance.[12,34] Accordingly, treatment with anti-programmed cell death protein 1 (PD-1) antibodies synergized with CARMA1 deficiency in Tregs, producing pronounced antitumor effects.

The mucosa-associated lymphoid tissue lymphoma translocation protein 1 (MALT1) has attracted special attention because it not only acts as a molecular scaffold to induce NF-κB signaling but also confers druggable proteolytic activity to the assembled CBM complex.[30] MALT1 paracaspase cleaves substrates that modulate signaling pathways (eg, cylindromatosis [CYLD], A20, and heme-oxidized IRP2 ubiquitin ligase 1), regulate transcription (transcription factor RelB), and stabilize RNA (eg, Regnase-1, Roquins).[30,35–37] Selective genetic destruction of MALT1 catalytic activity, but not its scaffold function, in Tregs severely impairs their immune-regulatory activity and triggers autoimmunity.[32,38] However, short-term pharmacological inhibition with the allosteric MALT1 inhibitor mepazine racemate[39,40] did not cause autoimmunity but produced antitumor effects similar to those of genetic BCL10 or CARMA1 deficiency.[32,34] Furthermore, mepazine treatment provoked proinflammatory Treg reprogramming, induced IFNγ-regulated gene expression in the TME, and, similar to CARMA1 deficiency, synergized with anti-PD-1 therapy.

These findings suggest that mepazine may afford a clinical benefit for the treatment of solid tumors as monotherapy and in combination with ICT. Herein we report findings from preclinical studies of the clinical drug candidate (*S*)-mepazine, which has approximately 10-fold greater MALT1 inhibitory activity than its *R* enantiomer.[40] The studies, including ex vivo analyses of murine and patient-derived tumor spheroids and in vivo pharmacological studies in murine tumor models, which were conducted with and without anti-PD-1 ICT, and biochemical and pharmacokinetic (PK) profiling, provide translational support for the first-in-human study of MPT-0118, (*S*)-mepazine succinate (ClinicalTrials.gov Identifier: NCT04859777).

MATERIALS AND METHODS

Patient tumor samples for organotypic spheroids were collected and analyzed according to Dana-Farber/Har-

vard Cancer Center (DF/HCC) institutional review board (IRB)-approved protocols. A cohort of patients (see Supplemental Table S1, available online) treated at Massachusetts General Hospital was assembled for PDOTS (patient-derived organotypic spheroids) profiling. These studies were conducted according to the Declaration of Helsinki and approved by the DF/HCC IRB. All patients provided written informed consent.

Animal experiments were conducted in accordance with the National Institutes of Health Guide for the Care and Use of Laboratory Animals and approved by Rincon Bio's Institutional Animal Care and Use Committee.

Studies were conducted using (*S*)-mepazine as either the succinate or hydrochloride salt (MPT-0118 and MPT-0308, respectively). Both salt forms were synthesized using methods similar to the published procedure.[40] Anti-mouse PD-1 antibody (29F.1A12) was procured through Bio X Cell (Lebanon, NH) and formulated in In Vivo Pure pH 7.0 Dilution Buffer.

In Vivo Studies in Murine MC38, D4M.3A, and B16.F10 Syngeneic Tumor Models

Animals

Animals were 6-week-old male C57BL/6J mice (Jackson Laboratory; Bar Harbor, ME; see Supplemental Material for animal care).

Tumor implantation

Tumor cells (see Supplemental Material for sources and preparation) were trypsinized and allowed to detach from flasks. Trypsin was then neutralized with complete media, cells were spun at 400*g* for 5 minutes, and media supernatant was aspirated. Cells were resuspended in 50:50 Cultrex:phosphate-buffered saline (PBS) (MC38) or washed with PBS and resuspended in PBS (D4M.3A) or Hank's balanced salt solution (HBSS) (B16.F10) (PBS [without Ca, Mg] and HBSS were purchased from Sigma-Aldrich, St. Louis, MO). Cell suspensions were injected into the right hind flank of each animal (1×10^6 cells [MC38, D4M.3A] or 0.5×10^6 cells [B16.F10]).

Treatment

(*S*)-mepazine was administered once daily by intraperitoneal (IP) injection (27-gauge needle) or oral gavage (nylon feeding needles [Instech Labs, Plymouth Meeting, PA]) beginning 7, 8, or 9 days after tumor implantation (B16.F10, MC38, and D4M.3A, respectively). Three doses of 200 μg anti-mouse PD-1 were administered IP 6 hours after (*S*)-mepazine injection every other day.

Tumor measurement

Tumors were measured with a digital caliper in two dimensions, and volume (mm^3) was calculated as $w^2 \times l/2$ (*w,* width; *l,* length [mm]).

Flow Cytometry

Mouse tumor tissue samples

Male C57BL/6J mice implanted with the D4M.3A tumor cell line were treated with (*S*)-mepazine, anti-mouse PD-1, or (*S*)-mepazine plus anti-mouse PD-1 as described above. In two experiments, MPT-0308 (32 mg/kg) was administered IP, and brefeldin A (500 μg [Sigma-Aldrich]) was injected together with the last treatment. Tumors were dissected 6 hours later, digested with DNAse I (Sigma-Aldrich) and collagenase, Type IV (Worthington Biochemical, Lakewood, NJ), and single-cell suspensions were prepared. Alternatively, MPT-0118 (64 mg/kg) was administered orally, and tumor samples were subsequently digested with DNAse I and collagenase IV in the presence of brefeldin A (2 μg/mL). Single-cell suspensions were then treated in vitro with brefeldin A (10 μg/mL) for 3 hours. Staining for Tregs (live $CD45^+$ $CD90.2^+$ $CD8^-$ $CD4^+$ $FoxP3^+$ cells) was performed, and the frequency of $IFN\gamma^+$ Tregs was analyzed by flow cytometry (anti-mouse antibodies CD45 PerCPCY5.5, CD90.2 AF488, CD8β BV510, and CD4 PacBlue were purchased from BioLegend [San Diego, CA], and anti-FoxP3, from eBioscience [San Diego, CA]).

Rat blood samples

Female Harlan Sprague Dawley rats (Envigo, Indianapolis, IN) were treated with MPT-0118 (30 mg/kg) once daily for 15 days (see Supplemental Material for animal care). During the study, blood samples were taken on days –1, 3, 5, 7, 10, and 14 from the same animals. After red blood cell lysis, the samples were stained with near-infrared fixable viability dye in combination with fluorescent antibodies to surface markers CD3, CD4, CD8α, and CD25 (all from BioLegend). After surface staining, the cells were fixed, permeabilized, and stained with anti-FoxP3 (eBioscience). The stained samples were then analyzed by flow cytometry (FlowJo software, Ashland, OR, versions 10.5.3 and 10.7.2) for the presence of Tregs ($CD3^+$ $CD4^+$ $CD8\alpha^-$ $FoxP3^+$).

Detection of CYLD cleavage by Western blotting in Jurkat T cells

Generation of MALT1-deficient Jurkat T cells has been previously described.[41] CYLD-deficient Jurkat T cells were generated by CRISPR-Cas9 technology as described in Meininger et al[41] using single guide RNAs directed against exon 8 of CYLD.[42] Jurkat T cells were stimulated for 2 h with phorbol 12-myristate 13-acetate (PMA; 200 ng/mL [Merck, Rahway, NJ]) and ionomycin (300 ng/mL [Calbiochem, San Diego, CA]), and CYLD cleavage was detected by anti-neoCYLDct antibody (clone 25F10 [see Supplemental Material on methods]) using Western blot. Anti-CYLD (E10; RRID: AB_1122022) for detection of cleaved and uncleaved CYLD, anti-MALT1 (B12; RRID: AB_627909), and anti-β-Actin (C4; RRID: AB_626632) antibodies were all purchased from Santa Cruz Biotechnology (Dallas, TX). Western blotting was performed as previously described.[43]

Organotypic Tumor Spheroids

Preparation and microfluidic culture

Murine-derived and patient-derived organotypic tumor spheroids (MDOTS/PDOTS) were prepared, cultured,

and characterized as previously described (summarized in the Supplemental Material).[44] Immune cells were present from the initial tumor resection, and spheroid-collagen mixtures (10 μL, 2.5 mg/mL tumor spheroids) were injected into the center gel region of the AIM Dax-01 3D microfluidic culture device (AIM Biotech, Singapore). After incubation (30 minutes at 37°C) in sterile humidity chambers, collagen hydrogels containing MDOTS/PDOTS were hydrated with media (Dulbecco's modified Eagle's medium), with or without the indicated treatments. Treatments included the antibodies anti-human IFNγ (10 μg/mL), anti-mouse IFNγ (10 μg/mL) (both from Bio X Cell), anti-human PD-1 (pembrolizumab), and (*S*)-mepazine. Murine D4M.3A-derived tumor spheroids and MDOTS were cultured ex vivo with MPT-0308 (0.3–10 μM) for 4 days, and murine MC38-derived MDOTS were cultured with MPT-0308 (3 μM ± anti-mouse IFNγ) or anti-mouse IFNγ alone for 6 days. PDOTS established from patients with colorectal cancer (CRC) and melanoma were cultured ex vivo with MPT-0118 or MPT-0308 (3–5 μM [unless otherwise specified] ± anti-PD-1 [pembrolizumab]) for 5 to 7 days; one experiment additionally included each treatment plus or minus anti-human IFNγ.

Viability assessment of MDOTS/PDOTS

Dual-label fluorescence-live/dead staining used Hoechst 33342/propidium iodide (Ho/PI) staining solution (Nexcelom, Lawrence, MA), as previously described.[44,45] Images were obtained following incubation with Ho/PI (45 minutes, 37°C, 5% CO_2), and image capture and analysis was performed using a Nikon (Tokyo, Japan) Eclipse NiE fluorescence microscope equipped with a motorized stage (ProScan; Prior, Cambridge, UK) and ZYLA 4.2 Plus USB3 Camera (Andor, Belfast, North Ireland) and NIS-Elements AR software package (version 5.40.00; Nikon Corporation). Live and dead cell quantitation was performed by measuring total raw cell area for each dye. Percent change and log2 fold change data were generated using raw fluorescence data (live) for the given treatments relative to control conditions.

Statistical Analyses

Statistical analyses were performed using GraphPad Prism (version 9.00 [GraphPad Software, San Diego, CA]). The two-tailed Student's *t* test was used for comparisons between two groups, and two-way ANOVA with Bonferroni or one-way ANOVA with the Tukey or Dunn post test were used for comparisons across multiple groups. Individual methods are described in the corresponding figure legends.

RESULTS

In Vivo Antitumor Effects in Murine Syngeneic Tumor Models

(*S*)-mepazine, alone or in combination with anti-PD-1, induces in vivo tumor-growth reduction and increases Treg fragility. As noted above, recent studies have shown moderate antitumor effects of racemic mepazine when used as a single agent, but pronounced synergistic activity in combination with anti-PD-1 ICT.[34] To assess the antitumor effects of the more active *S* enantiomer of mepazine, which shows 10-fold higher MALT1 inhibition than the *R* enantiomer[40] and may thus provide more selective pharmacodynamic effects than the racemate, we tested (*S*)-mepazine at different doses in several murine syngeneic tumor models. Because the hygroscopic properties of the HCl salt form of (*S*)-mepazine (MPT-0308) complicate long-term maintenance of medication quality, we also generated (*S*)-mepazine succinate (MPT-0118) for both oral and IP dosing. In the immunogenic MC38 model,[34,46] anti-PD-1 monotherapy afforded significant inhibition of tumor growth, as expected, as did single-agent MPT-0308 treatment (Fig. 1A). In contrast, two poorly immunogenic melanoma models (B16.F10 and D4M.3A[34,47,48]) were less responsive to anti-PD-1 monotherapy but consistently responded to high doses of MPT-0118 or MPT-0308 (Figs. 1B–D). The combination of anti-PD-1 with high dose of MPT-0308 had an additive effect in immunogenic MC38 tumors that already responded well to anti-PD-1 monotherapy (Fig. 1A), whereas clear synergy was observed with MPT-0118 or MPT-0308 in both poorly immunogenic models (Figs. 1B–D). Of note, we examined the pharmacodynamic similarity of MPT-0118 and MPT-0308 by administering both salt forms via the IP route in D4M.3A tumor-challenged mice and observed comparable effects on tumor growth (Supplemental Figs. S1A, B).

To assess if MPT-0118 pretreatment could enhance the synergistic antitumor effects achieved with anti-PD-1 by priming tumors for ICT, we compared combination therapy with and without 3-day lead-in MPT-0118 monotherapy (Supplemental Fig. S1C). Both regimens afforded similar antitumor effects, suggesting that pretreatment with MPT-0118 is a viable option, but it does not increase the combinatory effects achieved with simultaneous administration of MPT-0118 and anti-PD-1.

To examine whether MPT-0118 or MPT-0308 antitumor activity results from proinflammatory Treg reprogramming, Tregs from D4M.3A-challenged mice were analyzed for intratumoral infiltration and in situ IFNγ cytokine expression. The frequency of Treg among $CD45^+$ and $CD4^+$ cells was similar in all conditions (Figs. 2A, B), whereas the frequency of $IFN\gamma^+$ Tregs in mice treated with MPT-0118 or MPT-0308 monotherapy (7.1 ± 0.86%) or combination therapy with anti-PD-1 (8.9 ± 1.01%) was significantly increased in comparison with that of the vehicle-treated group (3.6 ± 0.54%; Fig. 2C). Mice treated with combination therapy also had a significantly greater frequency of $IFN\gamma^+$ Tregs than those treated with anti-PD-1 monotherapy (5.1 ± 0.71%), whereas no difference between control and

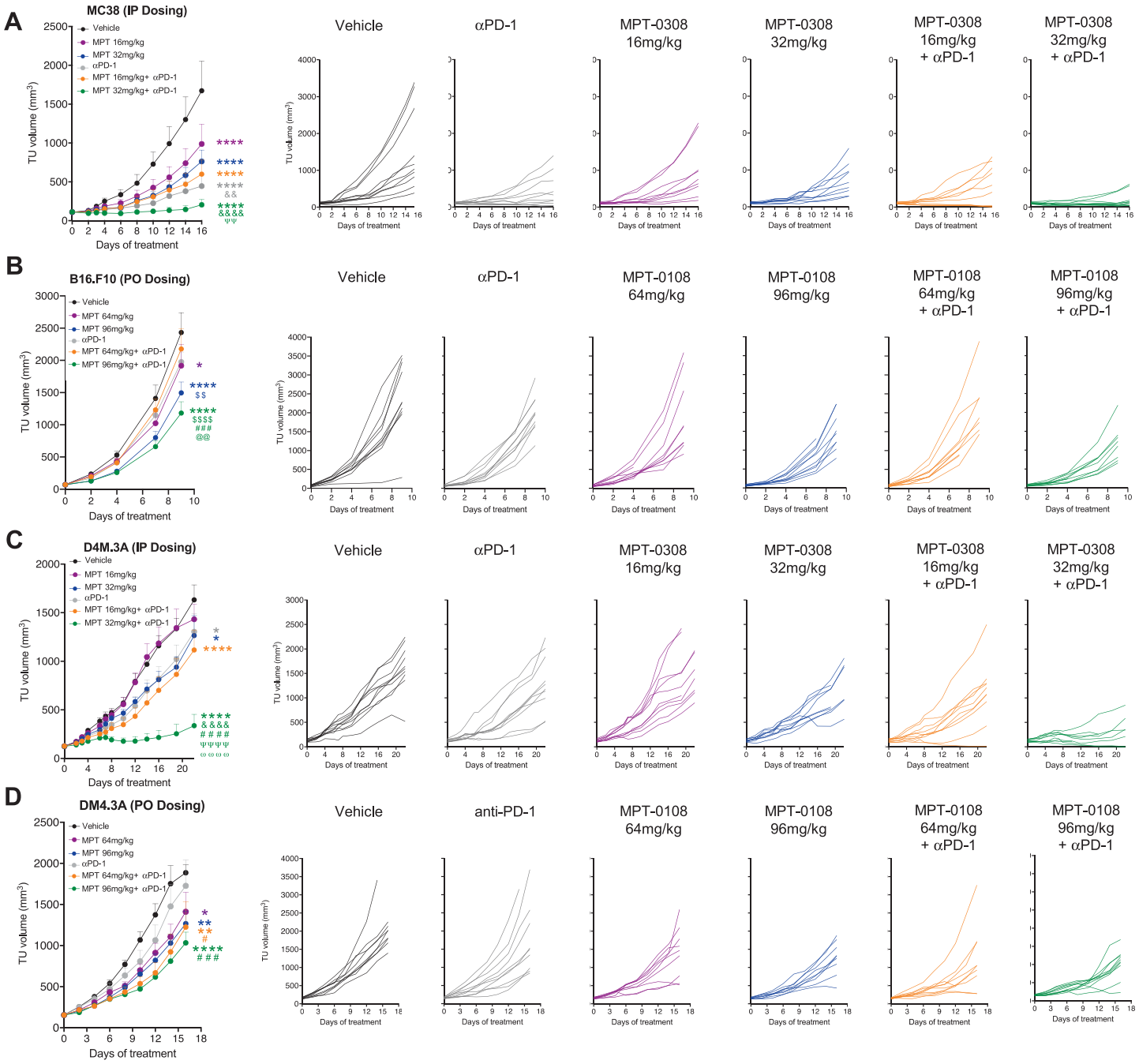

Figure 1. Tumor growth in murine tumor models dosed with (*S*)-mepazine, αPD-1, or a combination of both treatments.

A–D: Tumor-growth inhibition *p*-values are for the last day of treatment. Results are expressed as mean ± SEM. Statistical analyses: two-way ANOVA with Bonferroni post hoc test, $n = 10$ male C57BL/6J mice per cohort. Peritoneally infiltrated tumors are included; mice with early mortality are excluded (**A** and **D**: $n = 2$); missing data were not imputed.

Statistical differences are indicated as follows: *: any treatment group vs vehicle; #: any treatment group vs αPD-1; &: any treatment group vs MPT 16 mg/kg IP; ψ: any treatment group vs MPT 32 mg/kg IP; $: any treatment group vs MPT 64 mg/kg PO + αPD-1; @: any treatment group vs MPT 64 mg/kg PO; ω: any treatment group versus MPT 16 mg/kg IP + αPD-1.

Single symbol: $p < 0.05$; double symbol: $p < 0.01$; triple symbol: $p < 0.001$; quadruple symbol: $p < 0.0001$.

αPD-1: anti-programmed cell death protein 1; IP: intraperitoneal; PO: oral; TU: tumor.

the anti-PD-1-treated group was detected (Fig. 2C). Importantly, higher cytokine expression on Tregs correlated with diminished tumor growth across all (*S*)-mepazine–treated groups (Fig. 2D). Furthermore, because Treg reprogramming has been associated with a decrease or loss of FoxP3,[8,34] we analyzed the FoxP3 expression in total, IFNγ$^-$, and IFNγ$^+$ Tregs in each treated group. Although we noted no differences in the

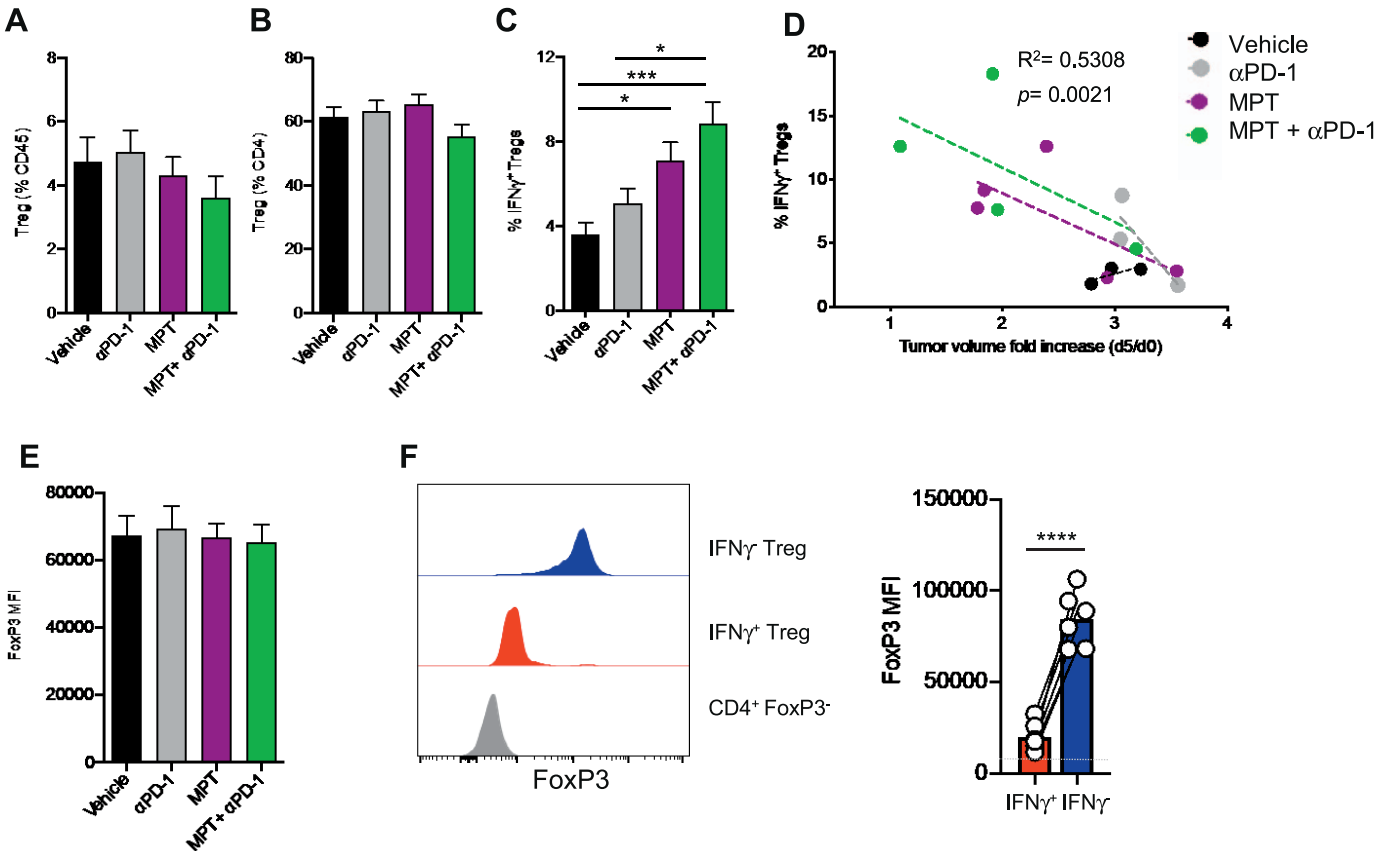

Figure 2. Infiltration, IFNγ, and FoxP3 expression in Tregs from mice dosed with (*S*)-mepazine, αPD-1, or a combination of both treatments.

A and **B:** Flow cytometry assessment of the frequency of tumor Tregs as percentage of (**A**) CD45 and (**B**) CD4.

C: IFNγ$^+$ Tregs as a percentage of total tumor-infiltrating Tregs in D4M.3A-injected mice after treatment with MPT-0118 or MPT-0308, αPD-1 (2 × 200 μg per day), or the combination. Pooled results are expressed as mean ± SEM. Statistical analyses: one-way ANOVA with Tukey post hoc test, number of tumors analyzed (n) = 13 (vehicle), n = 14 (αPD-1), n = 16 (10 MPT-0118, 6 MPT-0308), and n = 16 (MPT+ αPD-1) with *$p < 0.05$, ***$p < 0.001$.

D: Correlation between tumor growth and frequency of IFNγ$^+$ Tregs in D4M.3A-injected mice treated for 7 days with MPT-0118. Tumor volume fold change was determined as a ratio of tumor volume at day 5 to that at day 0 of treatment. The R^2 and p-value represent the overall correlation across groups.

E: Median fluorescent intensity of FoxP3 from total Treg.

F: Flow cytometry analysis gating scheme and median fluorescent intensity from IFNγ$^+$ and IFNγ$^-$ Treg from (*S*)-mepazine–treated mice. Dashed line indicates FoxP3 MFI in CD4$^+$ T conventional cells.

Statistical analyses: Student's paired t test (****$p < 0.0001$).

αPD-1: anti-programmed cell death protein 1; IFN: interferon; Treg: T regulatory cell.

total expression of FoxP3 in total Treg under each condition (Fig. 2E), we observed a significant, approximately four fold decrease of FoxP3 protein in those Tregs that express IFNγ compared with those that do not (Fig. 2F).

Overall, these results indicate that both IP and oral treatment with the MALT1 inhibitor (*S*)-mepazine inhibits the growth of poorly immunogenic tumors and renders them more susceptible to ICT. The findings further suggest that the observed antitumor effects of (*S*)-mepazine correlate with Treg reprogramming from a stable, suppressive phenotype to a "fragile," proinflammatory phenotype.

(S)-Mepazine Properties and Tumor Accumulation

(*S*)-mepazine has favorable tumor accumulation with a peak concentration that efficiently blocks MALT1 activity. (*S*)-mepazine belongs to the class of phenothiazine drugs, and acts as a moderately potent, reversible, noncompetitive, allosteric inhibitor of MALT1 protease function.[39,40] As a lipophilic basic amine molecule, (*S*)-mepazine exhibited an octanol–water partition coefficient (logP) of 5.29 and pKa of 9.2 with apparent pH-dependent solubility. The mean apparent AB permeability coefficient in a Caco-2 assay was 13.73 ± 0.15 × 10^{-6} cm/s, and the drug was not a P-gp substrate (Supple-

mental Table S2). These data indicate that (*S*)-mepazine has good cell permeability and cell retention.

Despite its lower potency compared with other MALT1 inhibitors currently in preclinical or clinical development,[49,50] (*S*)-mepazine, as either the succinate or hydrochloride salt (MPT-0118 and MPT-0308, respectively), demonstrated remarkable effects on tumor control. To evaluate whether its antitumor activity is potentially supported by favorable tumor tissue distribution, we assessed its PK properties. (*S*)-mepazine demonstrated suitable PK in non–tumor-bearing animals (Supplemental Table S3). It was readily absorbed into the systemic circulation (Tmax generally within 2 hours) and demonstrated broad tissue distribution in rats and mice (Supplemental Table S4). MPT-0118 also displayed favorable tumor distribution in D4M.3A tumor-bearing mice (Fig. 3A). Notably, when MPT-0118 was orally administered at 64 mg/kg/day at steady-state (following 21 days of consecutive treatment), peak concentrations in mouse plasma remained relatively low ($\leq$1.3 μM), whereas consistently higher drug concentrations (3–10 μM) were observed in tumor tissue over the following 24 hours.

To determine if drug concentrations observed in tumor tissue are sufficient to achieve robust MALT1 inhibition, we developed an assay to quantify MALT1 protease function by measuring the cleavage of its CYLD substrate[51] in T cells in vitro. To directly assess the CYLD cleavage product (CYLD-ct), we raised the monoclonal antibody clone 25F10, which reacts with a neoepitope of both the human and mouse CYLD C-terminal cleavage products (Fig. 3B). The anti-neoCYLD-ct antibody also detects the appearance of the CYLD cleavage product upon MALT1 activation in single-cell flow cytometry (Figs. 3C, E). Drug titration on activated human Jurkat cells revealed a sigmoidal dose-response pattern and complete MALT1 inhibition at a dose between 10 and 30 μM (half-maximal inhibitory concentration [IC_{50}] = 3.9 μM; Figs. 3C, D). In murine splenic $CD4^+$ T cells stimulated with PMA/ionomycin, MPT-0308 showed half-maximal MALT1 inhibition at 1.132 μM (Fig. 3F), which was above the maximal plasma concentrations observed at steady-state in mice on therapeutic dose levels. At concentrations of 3 and 10 μM, which approximated the range observed in tumor tissue at steady-state, MALT1 was inhibited by roughly 75% and 95%, respectively (Figs. 3E, F). Thus, pharmacodynamic profiling revealed favorable bio-distribution of (*S*)-mepazine to the targeted tumor with concentrations that are likely sufficient to strongly inhibit MALT1 protease activity in vivo.

Effects of (S)-Mepazine on Tregs in Rats

In non–tumor-bearing rats, (*S*)-mepazine does not cause significant changes in Treg frequencies. Because high-potency MALT1 inhibitors induce Treg depletion associated with autoimmune toxicity,[50] we explored whether effective doses of MPT-0118 have similar effects. Non–tumor-bearing female rats were treated daily with 30 mg/kg of orally administered MPT-0118, which, based on allometric scaling and PK assessments, corresponds to the mouse oral dose of 64 mg/kg. No change in circulating Treg frequencies was observed over 15 days for MPT-0118–treated rats compared with vehicle-treated animals (Fig. 4). These results show that treatment with (*S*)-mepazine at doses efficacious in tumor-bearing mice does not affect Treg frequencies in peripheral blood, suggesting that potential systemic autoimmune toxicity can be avoided.

Assessment of (S)-Mepazine in MDOTS and PDOTS

(*S*)-mepazine enhances sensitivity to PD-1 blockade in organotypic tumor spheroids. It is unknown whether, similar to mouse Tregs, human tumor-infiltrating Tregs can be reprogrammed into proinflammatory cells through MALT1 inhibition. We therefore adopted the PDOTS model, which provides the opportunity to examine the response of cancer and immune cells to drug treatments ex vivo in a partially preserved human TME in a microfluidic chamber.[44,45] First, to test whether organotypic tumor spheroids reproduce the microenvironmental conditions of the TME that support Treg reprogramming, we generated MDOTS from murine D4M.3A tumors grown in mice. Although the viability of ex vivo aggregated tumor spheroids that lacked immune cells and a tumor stroma was not affected by MPT-0308 treatment at doses up to 10 μM, MDOTS showed a dose-dependent reduction in viability, starting at a dose between 1 and 3 μM (Supplemental Figs. S2A, B). We confirmed that 3 μM MPT-0308 was also active using a different murine tumor model (MC38) and found that the antitumor activity could be reversed using an anti-IFNγ neutralizing antibody (Supplemental Fig. S2C). These observations suggest that organotypic tumor spheroids support proinflammatory Treg reprogramming at doses of MPT-0308 that have no direct effect on cancer cell viability.

Next, we generated PDOTS[44,45] from surgically resected tumor tissue from human patients with cutaneous melanoma, non-cutaneous melanoma, microsatellite instable (MSI) CRC, or microsatellite stable (MSS) CRC (Fig. 5A, Supplemental Table S1) and treated those with MPT-0118 or MPT-0308 monotherapy, anti-PD-1 monotherapy, or combination therapy. The response rate (response defined as $\geq$30% reduction in tumor cell viability) was numerically greater for the groups treated with MPT-0118 or MPT-0308 (3 of 13, 23.1%) or combination therapy (5 of 13, 38.5%) than for the anti-PD-1 monotherapy-treated group (2 of 13, 15.4%) and significantly higher in combination therapy samples compared with controls (Fig. 5B). PDOTS from patients with MSI and MSS CRC were among the most sensitive to MPT-0118 or MPT-0308 with or without anti-PD-1 treatment at either an intermediate dose (3–5 μM) (Fig. 5C, D) or a high dose (10 μM) (Fig. 5E). Importantly, IFNγ

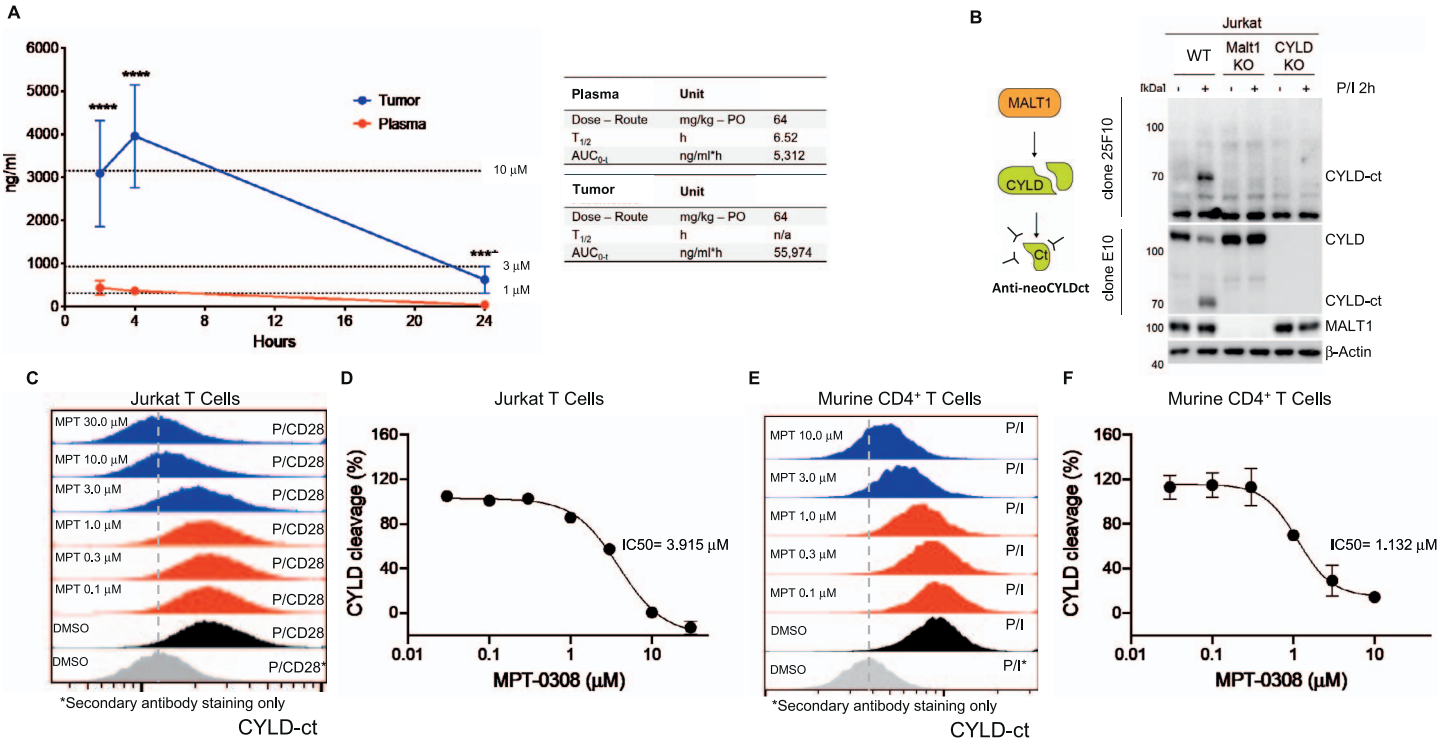

Figure 3. (*S*)-mepazine target engagement assessments: plasma/tumor pharmacokinetics in mice and cleavage assay of the MALT1 CYLD substrate in T cells.

A: Drug plasma and tumor concentrations in D4M.3A tumor-bearing C57BL/6J male mice treated with 64 mg/kg MPT-0118 at steady-state following pretreatment for 21 days. Statistical analyses: Student's unpaired *t* test, $n = 5$ mice per time point (****$p < 0.0001$).

B: Western blotting of CYLD and CYLD-ct from WT, MALT1 KO, and CYLD KO Jurkat T cells with and without stimulation. B-actin was used as the internal loading control. Antibody clone 25F10 recognizes a neoepitope of CYLD-ct (neoCYLDct; human and mouse), and clone E10 (control) recognizes both CYLD and CYLD-ct.

C: Flow cytometry analysis showing CYLD-ct in Jurkat T cells after treatment with MPT-0308 or DMSO and stimulation with PMA and CD28. Vertical dashed line indicates median fluorescence intensity of CYLD-ct in DMSO-treated cells.

D: Dose titration of MPT-0308 measuring MALT1-cleaved CYLD-ct in Jurkat T cells. Results are shown as mean ± SEM ($n = 4$).

E: Flow cytometry analysis showing CYLD-ct in murine $CD4^+$ T cells after treatment with MPT-0308 or DMSO and stimulation with PMA and ionomycin (I). Vertical dashed line indicates median fluorescence intensity of CYLD-ct in DMSO-treated cells.

F: Dose titration of MPT-0308 measuring MALT1-cleaved CYLD-ct in murine $CD4^+$ T cells. Results are shown as mean ± SEM ($n = 3$).

$AUC_{0\text{-}t}$: area under the concentration-time curve from time 0 to time t; CYLD: cylindromatosis; CYLD-ct: CYLD cleavage product; DMSO: dimethyl sulfoxide; IC50: half-maximal inhibitory concentration; KO: knockout; n/a: not available; PMA: phorbol 12-myristate 13-acetate; PO: oral; $t_{1/2}$, half-life; WT: wild type.

was required for the antitumor efficacy of MPT-0118 in combination with anti-PD-1 treatment, because effects on PDOTS could be reversed by addition of anti-IFNγ neutralizing antibody (Fig. 5F). Thus, MALT1 inhibition by (*S*)-mepazine was also efficacious in human tumor tissue ex vivo, both as monotherapy and by enhancing the effects of PD-1 blockade, likely through proinflammatory effects induced by Treg reprogramming.

DISCUSSION

Herein we describe preclinical studies on MPT-0118 and MPT-0308, two orally available formulations of (*S*)-mepazine and allosteric inhibitors of MALT1 protease function, extending recent findings demonstrating the antitumor effects of mepazine racemate and its capacity to prime unresponsive tumors for ICT.[34] The mechanistic hypothesis purports a role for the selective reprogramming of immunosuppressive Tregs in the TME into fragile, IFNγ-secreting, proinflammatory antitumor effector cells. In line with this hypothesis, both formulations of (*S*)-mepazine demonstrated significant antitumor effects that were synergistic with anti-PD-1 therapy and positively correlated with the amount of IFNγ secretion by tumor-associated Tregs. Pharmacokinetic profiling revealed favorable accumulation of MPT-0118 in tumor tissue, which likely supports its selective pharmacodynamic effects, avoiding the systemic autoimmune toxicity associated with more potent and symmetrically distributed MALT1 inhibitors.[50] Finally,

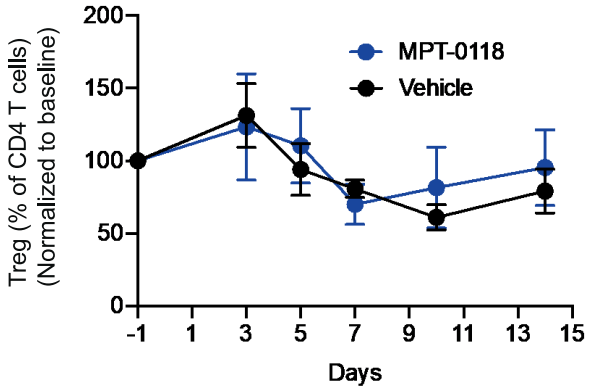

Figure 4. Effect of MPT-0118 (30 mg/kg, every day, orally) administered for 15 days on circulating Tregs in blood samples from female Harlan Sprague Dawley rats, assessed by flow cytometry. The data represent the frequency of circulating Tregs as a percentage of $CD4^+$ T cells vs baseline (data are normalized to the baseline values [defined as 100%]). The 30 mg/kg oral dose corresponds to the 64 mg/kg oral efficacious dose used in mouse studies.

Results are expressed as mean ± SEM. Student's unpaired *t* test was applied for statistical analysis of single time points vs cohort baseline at day −1 ($n = 5$ per cohort).

studies in (*S*)-mepazine–treated human organotypic tumor spheroids suggested that Treg reprogramming can also occur in the TME of human patients with cancer and exert antitumor activity.

In both immunogenic and poorly immunogenic tumor models,[46–48] (*S*)-mepazine demonstrated significant in vivo tumor-growth reduction, and antitumor effects were sustained over the dosing interval. Tumor-growth deceleration by (*S*)-mepazine was dose dependent, and in some cases, the effects of higher-dose single-agent treatment were greater than the effects achieved with anti-PD-1 monotherapy. Moreover, combinatory high-dose (*S*)-mepazine plus anti-PD-1 treatment consistently showed superior antitumor activity compared with anti-PD-1 monotherapy in poorly immunogenic tumors. Notably, the frequency of $IFN\gamma^+$ Tregs inversely correlated with tumor growth, supporting the proposed mechanism of Treg reprogramming. These findings further characterize the in vivo effects of (*S*)-mepazine, building on the evidence established with racemic mepazine.[32,34]

Disruption of the CBM signalosome complex, in particular its MALT1 protease function, is an attractive approach for manipulating Tregs in the TME, as MALT1 is essential to Treg suppressive function.[32] Furthermore, selective targeting of tumor-associated Tregs has been observed with MALT1 inhibition, likely due to a particular dependence of Tregs on MALT1 function in the metabolic and inflammatory milieu of the TME of solid tumors.[34] Germline deficiency of MALT1 protease function in mice causes reductions in the number of circulating Tregs and severe autoimmunity,[52–55] which raised concerns regarding the effects of long-term pharmacological inhibition. It was later shown that MALT1 protease deficiency, when induced in adult mice, did not cause autoimmune toxicity despite a similar reduction in Tregs.[56] A limitation of this study was that genetic MALT1 inactivation may not have been complete, and residual MALT1 protease-sufficient Tregs might have sufficed to maintain immune homeostasis. This scenario, however, likely compares with incomplete pharmacological MALT1 inhibition. In fact, while efficacious treatment with the highly potent MALT1 inhibitor MLT-943 ($IC_{50} < 10$ nM) caused rapid reduction of Tregs in rats and dogs (maximal after 7 days in rats) with subsequent development of a reversible immune dysregulation, polyendocrinopathy, enteropathy, X-linked (IPEX)-like pathology in rats,[50] Treg reduction was dose-dependent and less pronounced or absent at lower concentrations that were, however, still affecting T-cell effector responses.[57] In our study, treatment of rats for 15 days with the moderately potent inhibitor MPT-0118 at 30 mg/kg (orally), a dose corresponding to an efficacious dose in mice, had no effect on Treg frequencies in peripheral blood, similar to previous findings in mice treated with mepazine racemate at doses of 8 mg/kg (twice a day, IP) and 16 mg/kg (every day, IP).[50,58]

We hypothesized that the apparent lack of systemic effects of (*S*)-mepazine on Tregs may be due in part to its favorable tumor distribution at the effective dose, as noted in murine syngeneic tumor models where peak concentrations in tumor tissue at steady-state remained well above those in plasma over the observation period. The pK of (*S*)-mepazine, and consequently its volume distribution, could explain its preferential accumulation in the highly perfused tumor tissue. Furthermore, amine-containing drugs are sequestered into acidic organelles and selective accumulation of lipophilic cations in cancer cells has been already shown, so the cationic and lipophilic nature of basic amine (*S*)-mepazine could also suggest some retention within tumor due to the acidification of the tumor microenvironment.[59,60]

To assess the degree of MALT1 inhibition achieved by drug levels measured in tumors, we generated an antibody against the human and murine cleavage product of the MALT1 protease substrate CYLD. Using this reagent, which may provide for a convenient pharmacodynamic biomarker in clinical MALT1 inhibitor studies for various indications, we showed that steady-state tumor drug levels at therapeutic doses inhibited MALT1 protease by 75% to 95%. The fact that such partial inhibition produced pronounced antitumor effects parallels prior observations whereby a partial reduction of CARMA1 protein was sufficient to reprogram tumor-infiltrating Tregs but did not affect Tregs elsewhere or cause autoimmune disease.[34–61] This supports the concept that incomplete target occupancy is desirable in the use of MALT1 inhibitors for the immunotherapy of cancer, especially because it will also minimize any potential immune-suppressive effects on effector lymphocytes that could mitigate the antitumor immune response.

PD-L1 upregulation on tumor cells, triggered by IFNγ released by Treg cells in response to treatment with

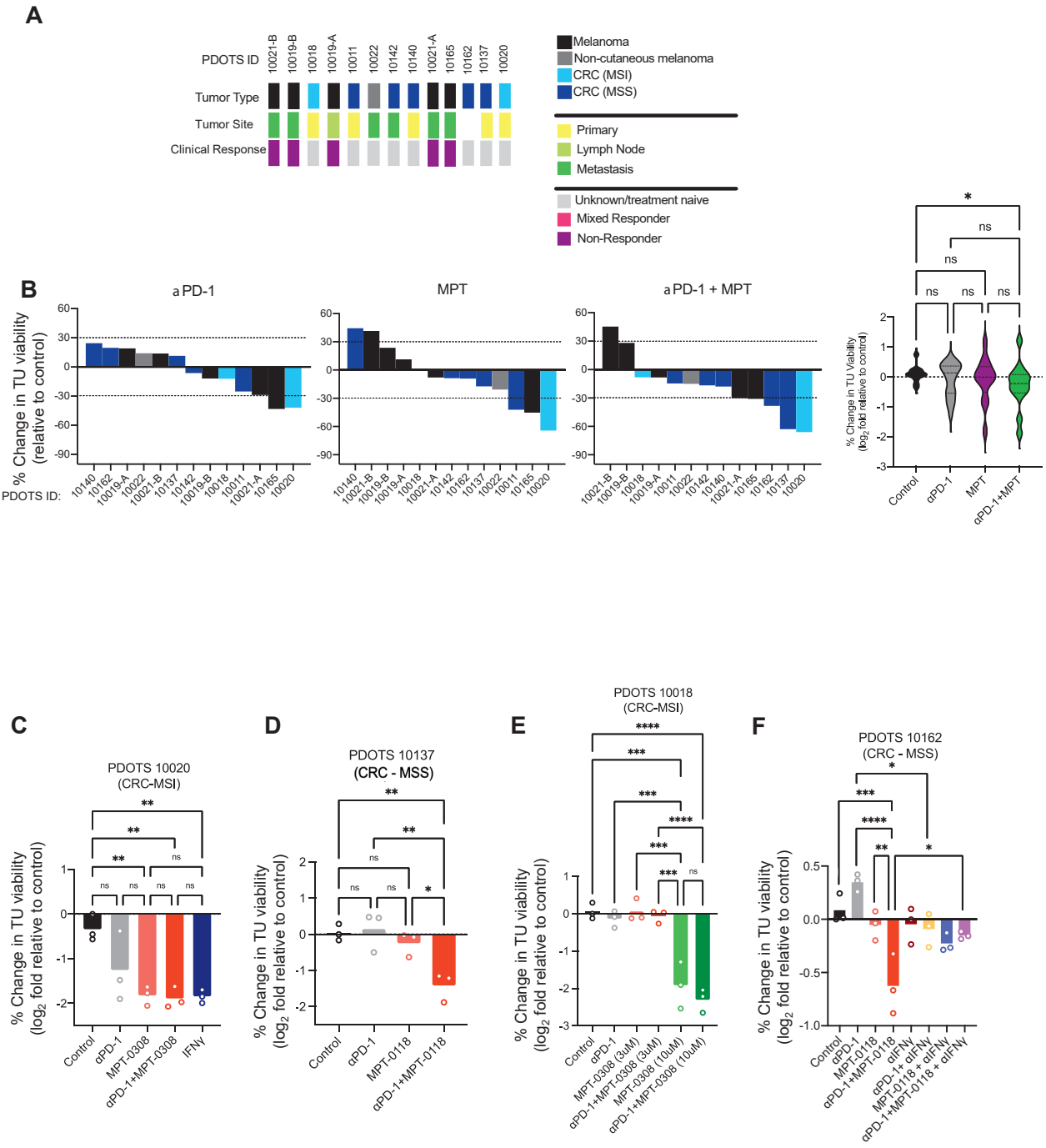

Figure 5. Patient-derived organotypic tumor spheroids treated with (*S*)-mepazine, αPD-1, or a combination of both treatments. Results are expressed as means.

A: Tumor type, tissue source (location), and clinical response data. Samples ordered by ex vivo PDOTS response to combined αPD-1 + (*S*)-mepazine.

B: Waterfall plots for PDOTS ($n = 13$, indicated tumor types) treated with αPD-1 (pembrolizumab, 250 μg/mL), (*S*)-mepazine (MPT-0308 or MPT-0118, 3–5 μM), or both showing percentage change in cell viability relative to untreated control. Statistical analyses: one-way ANOVA for paired samples ($n = 13$ biological replicates).

C–F: PDOTS viability assessment from patients with exceptional response to (S)-mepazine. (**C**) MPT-0308 3 μM; (**D**, **F**) MPT-0118 5 μM; (**E**) MPT-0118 3 and 10 μM ± αPD-1 (250 μg/mL, pembrolizumab); (**C**) ± IFNγ (50 ng/mL); (**F**) in addition ± αIFNγ (10 μg/mL). Statistical analyses: Dunn multiple comparisons test ($n = 3$ biological replicates).

*$p < 0.05$; **$p < 0.01$; ***$p < 0.001$; ****$p < 0.0001$.

αIFNγ: anti-interferon-γ; αPD-1: anti-programmed cell death protein 1; CRC, colorectal cancer; ID: identification; IFN: interferon; MSI, microsatellite instable; MSS, microsatellite stable; ns: not significant; PDOTS: patient-derived organotypic spheroids; TU: tumor.

mepazine racemate, likely limits the drug's single-agent antitumor activity, and explains the synergy with anti-PD-1 immunotherapy.[34] MPT-0118 and MPT-0308 treatment also significantly improved the effectiveness of anti-PD-1 ICT in poorly immunogenic models, which was less pronounced in immunogenic MC38 tumors that already responded well to anti-PD-1 monotherapy. We also investigated the priming effect of lead-in treatment with MPT-0118 followed by MPT-0118 plus anti-PD-1 in the D4M.3A model. Lead-in MPT-0118 monotherapy preserved the synergistic effects demonstrated by simultaneous initiation of both agents. Lead-in MPT-0118 priming could be further explored using biomarkers to monitor tumor inflammation and identify optimal time points for the initiation of combination treatment.

An abundance of immunosuppressive Tregs in the TME commonly constrains the effectiveness of ICT. Successful proinflammatory reprogramming can turn Tregs from a liability into an asset to prime the TME for immunotherapy. Multiple studies have reported similar effects on tumor-associated Tregs through various interventions targeting mechanisms implicated in maintaining their suppressive function in the TME.[22–28] A common denominator of these interventions is that they elicit Treg secretion of IFNγ. Of note, spontaneous, basal IFNγ secretion by tumor-infiltrating Tregs may even be a prerequisite for response to ICT, as anti-PD-1 blockade loses its efficacy in animals whose Tregs are genetically deficient in IFNγ expression.[62] We found that Treg expression levels of IFNγ inversely correlated with tumor growth and that IFNγ was critical to the ex vivo antitumor effects of MPT-0118 and MPT-0308 in PDOTS, suggesting that inflammatory Treg reprogramming was involved.

Overall, findings from the studies reported herein further support Treg reprogramming as a mechanistically informed approach to immunotherapy either alone or in concert with ICT. However, gaps remain in our understanding of how MALT1 inhibition induces Treg reprogramming from a suppressive to a proinflammatory cell state. Also unclear is whether PK distribution in patients will track with findings from the murine studies. Furthermore, the safety and tolerability of MPT-0118 and its antitumor effects in the clinic remain to be characterized along with key biomarkers for in-depth mechanistic investigations. These limitations are being addressed in ongoing studies, including a phase 1/1b dose-escalation and cohort expansion clinical trial, which was initiated in April 2021 (ClinicalTrials.gov Identifier: NCT04859777).

CONCLUSION

(*S*)-mepazine, a moderately potent inhibitor of MALT1 protease function, demonstrated promising efficacy in syngeneic tumor models and human cancer specimens, potentially mediated by tumor-associated proinflammatory Treg reprogramming and enabled in part by distinctive PK properties supporting favorable tumor accumulation. The translational aspects of this research supported initiation of the first-in-human study of MPT-0118, both as monotherapy and in combination with pembrolizumab in patients with advanced or metastatic refractory solid tumors.

Acknowledgments

We thank Kerstin Kutzner, Andrew Flatley, and Aloys Schepers (Helmholtz Munich–German Research Center for Environmental Health, Neuherberg, Germany) for excellent technical assistance and Tina Morwick (Consultant to Monopteros Therapeutics) for medical writing assistance.

Portions of this work were presented at the following conferences:

- ESMO Annual Conference, Sep 16–21, 2021, Virtual, Abstract 1020P
- AACR-NCI-EORTC Molecular Targets and Cancer Therapeutics, Oct 7–10, 2021, Virtual, Abstract P106
- SITC Annual Conference, Nov 12–14, 2021, Washington DC, Abstract 861
- SITC Tumor Immune Microenvironment: A holistic approach, Apr 21–22, 2022, San Diego, Abstracts 037 and 042

Supplemental Material

Supplemental materials are available online with the article.

References

1. Teh PP, Vasanthakumar A, Kallies A. Development and function of effector regulatory T cells. *Prog Mol Biol Transl Sci*. 2015;136:155–174.
2. Hatzioannou A, Boumpas A, Papadopoulou M, et al. Regulatory T cells in autoimmunity and cancer: a duplicitous lifestyle. *Front Immunol*. 2021;12:731947.
3. Campbell DJ, Koch MA. Phenotypical and functional specialization of FOXP3+ regulatory T cells. *Nat Rev Immunol*. 2011;11:119–130.
4. Tanaka A, Sakaguchi S. Regulatory T cells in cancer immunotherapy. *Cell Res*. 2017;27:109–118.
5. Tanaka A, Sakaguchi S. Targeting Treg cells in cancer immunotherapy. *Eur J Immunol*. 2019;49:1140–1146.
6. Ohue Y, Nishikawa H. Regulatory T (Treg) cells in cancer: can Treg cells be a new therapeutic target? *Cancer Sci*. 2019;110:2080–2089.
7. Scott EN, Gocher AM, Workman CJ, Vignali DAA. Regulatory T cells: barriers of immune infiltration into the tumor microenvironment. *Front Immunol*. 2021;12:702726.
8. Overacre-Delgoffe AE, Vignali DAA. Treg fragility: a prerequisite for effective antitumor immunity? *Cancer Immunol Res*. 2018;6:882–887.
9. Liu C, Workman CJ, Vignali DA. Targeting regulatory T cells in tumors. *FEBS J*. 2016;283:2731–2748.

10. Dees S, Ganesan R, Singh S, Grewal IS. Regulatory T cell targeting in cancer: emerging strategies in immunotherapy. *Eur J Immunol*. 2021;51:280–291.
11. Li C, Jiang P, Wei S, Xu X, Wang J. Regulatory T cells in tumor microenvironment: new mechanisms, potential therapeutic strategies and future prospects. *Mol Cancer*. 2020;19:116.
12. Sharma P, Hu-Lieskovan S, Wargo JA, Ribas A. Primary, adaptive, and acquired resistance to cancer immunotherapy. *Cell*. 2017;168:707–723.
13. Principe DR, Chiec L, Mohindra NA, Munshi HG. Regulatory T-cells as an emerging barrier to immune checkpoint inhibition in lung cancer. *Front Oncol*. 2021;11:684098.
14. Saman H, Uddin S, Raza S, Shrimali R, Rasul K. Understanding checkpoint inhibitors in cancer therapy, mechanisms of action, resistance and future challenges. *Clin Oncol Res*. 2020;3:2–13.
15. Ribas A, Wolchok JD. Cancer immunotherapy using checkpoint blockade. *Science*. 2018;359:1350–1355.
16. Twomey JD, Zhang B. Cancer immunotherapy update: FDA-approved checkpoint inhibitors and companion diagnostics. *AAPS J*. 2021;23:39.
17. Zhao B, Zhao H, Zhao J. Efficacy of PD-1/PD-L1 blockade monotherapy in clinical trials. *Ther Adv Med Oncol*. 2020;12:1758835920937612.
18. O'Donnell JS, Long GV, Scolyer RA, Teng MW, Smyth MJ. Resistance to PD1/PDL1 checkpoint inhibition. *Cancer Treat Rev*. 2017;52:71–81.
19. Kamada T, Togashi Y, Tay C, et al. PD-1^{+} regulatory T cells amplified by PD-1 blockade promote hyperprogression of cancer. *Proc Natl Acad Sci U S A*. 2019;116:9999–10008.
20. Munn DH, Sharma MD, Johnson TS. Treg Destabilization and reprogramming: implications for cancer immunotherapy. *Cancer Res*. 2018;78:5191–5199.
21. Dixon ML, Leavenworth JD, Leavenworth JW. Lineage reprogramming of effector regulatory T cells in cancer. *Front Immunol*. 2021;12:717421.
22. Nakagawa H, Sido JM, Reyes EE, Kiers V, Cantor H, Kim HJ. Instability of Helios-deficient Tregs is associated with conversion to a T-effector phenotype and enhanced antitumor immunity. *Proc Natl Acad Sci U S A*. 2016;113:6248–6253.
23. Overacre-Delgoffe AE, Chikina M, Dadey RE, et al. Interferon-γ drives T_{reg} fragility to promote anti-tumor immunity. *Cell*. 2017;169:1130–1141.e11.
24. Amoozgar Z, Kloepper J, Ren J, et al. Targeting Treg cells with GITR activation alleviates resistance to immunotherapy in murine glioblastomas. *Nat Commun*. 2021;12:2582.
25. Hatzioannou A, Banos A, Sakelaropoulos T, et al. An intrinsic role of IL-33 in T_{reg} cell-mediated tumor immunoevasion. *Nat Immunol*. 2020;21:75–85.
26. Dixon ML, Luo L, Ghosh S, Grimes JM, Leavenworth JD, Leavenworth JW. Remodeling of the tumor microenvironment via disrupting Blimp1^{+} effector Treg activity augments response to anti-PD-1 blockade. *Mol Cancer*. 2021;20:150.
27. Wang D, Quiros J, Mahuron K, et al. Targeting EZH2 reprograms intratumoral regulatory T cells to enhance cancer immunity. *Cell Rep*. 2018;23:3262–3274.
28. Grinberg-Bleyer Y, Oh H, Desrichard A, et al. NF-κB c-Rel is crucial for the regulatory T cell immune checkpoint in cancer. *Cell*. 2017;170:1096–1108.e13.
29. Rech AJ, Mick R, Martin S, et al. CD25 blockade depletes and selectively reprograms regulatory T cells in concert with immunotherapy in cancer patients. *Sci Transl Med*. 2012;4:134ra62.
30. Ruland J, Hartjes L. CARD-BCL-10-MALT1 signalling in protective and pathological immunity. *Nat Rev Immunol*. 2019;19:118–134.
31. Meininger I, Krappmann D. Lymphocyte signaling and activation by the CARMA1-BCL10-MALT1 signalosome. *Biol Chem*. 2016;397:1315–1333.
32. Rosenbaum M, Gewies A, Pechloff K, et al. Bcl10-controlled Malt1 paracaspase activity is key for the immune suppressive function of regulatory T cells. *Nat Commun*. 2019;10:2352.
33. Yang D, Zhao X, Lin X. Bcl10 is required for the development and suppressive function of Foxp3+ regulatory T cells. *Cell Mol Immunol*. 2021;18:206–218.
34. Di Pilato M, Kim EY, Cadilha BL, et al. Targeting the CBM complex causes T_{reg} cells to prime tumours for immune checkpoint therapy. *Nature*. 2019;570:112–116.
35. Juilland M, Thome M. Holding all the CARDs: how MALT1 controls CARMA/CARD-dependent signaling. *Front Immunol*. 2018;9:1927.
36. Jaworski M, Thome M. The paracaspase MALT1: biological function and potential for therapeutic inhibition. *Cell Mol Life Sci*. 2016;73:459–473.
37. O'Neill TJ, Seeholzer T, Gewies A, et al. TRAF6 prevents fatal inflammation by homeostatic suppression of MALT1 protease. *Sci Immunol*. 2021;6:eabh2095.
38. Cheng L, Deng N, Yang N, Zhao X, Lin X. Malt1 protease is critical in maintaining function of regulatory T cells and may be a therapeutic target for antitumor immunity. *J Immunol*. 2019;202:3008–3019.
39. Nagel D, Spranger S, Vincendeau M, et al. Pharmacologic inhibition of MALT1 protease by phenothiazines as a therapeutic approach for the treatment of aggressive ABC-DLBCL. *Cancer Cell*. 2012;22:825–837.
40. Schlauderer F, Lammens K, Nagel D, et al. Structural analysis of phenothiazine derivatives as allosteric inhibitors of the MALT1 paracaspase. *Angew Chem Int Ed Engl*. 2013;52:10384–10387.
41. Meininger I, Griesbach RA, Hu D, et al. Alternative splicing of MALT1 controls signalling and activation of CD4(+) T cells. *Nat Commun*. 2016;7:11292.
42. Lork M, Kreike M, Staal J, Beyaert R. Importance of validating antibodies and small compound inhibitors using genetic knockout studies-T cell receptor-induced CYLD phosphorylation by IKKε/TBK1 as a case study. *Front Cell Dev Biol*. 2018;6:40.
43. Kutzner K, Woods S, Karayel O, et al. Phosphorylation of serine-893 in CARD11 suppresses the formation and activity of the CARD11-BCL10-MALT1 complex in T and B cells. *Sci Signal*. 2022;15:eabk3083.
44. Jenkins RW, Aref AR, Lizotte PH, et al. *Ex vivo* profiling of PD-1 blockade using organotypic tumor spheroids. *Cancer Discov*. 2018;8:196–215.
45. Aref AR, Campisi M, Ivanova E, et al. 3D microfluidic ex vivo culture of organotypic tumor spheroids to model immune checkpoint blockade. *Lab Chip*. 2018;18:3129–3143.
46. Mosely SI, Prime JE, Sainson RC, et al. Rational selection of syngeneic preclinical tumor models for immunotherapeutic drug discovery. *Cancer Immunol Res*. 2017;5:29–41.
47. Lechner MG, Karimi SS, Barry-Holson K, et al. Immunogenicity of murine solid tumor models as a defining feature of in vivo behavior and response to immunotherapy. *J Immunother*. 2013;36:477–489.

48. Jenkins MH, Steinberg SM, Alexander MP, et al. Multiple murine BRaf(V600E) melanoma cell lines with sensitivity to PLX4032. *Pigment Cell Melanoma Res*. 2014;;27:495–501.
49. Bardet M, Unterreiner A, Malinverni C, et al. The T-cell fingerprint of MALT1 paracaspase revealed by selective inhibition. *Immunol Cell Biol*. 2018;96:81–99.
50. Martin K, Junker U, Tritto E, et al. Pharmacological Inhibition of MALT1 protease leads to a progressive IPEX-like pathology. *Front Immunol*. 2020;11:745.
51. Afonina IS, Elton L, Carpentier I, Beyaert R. MALT1—a universal soldier: multiple strategies to ensure NF-κB activation and target gene expression. *FEBS J*. 2015;282:3286–3297.
52. Jaworski M, Marsland BJ, Gehrig J, et al. Malt1 protease inactivation efficiently dampens immune responses but causes spontaneous autoimmunity. *EMBO J*. 2014;33:2765–2781.
53. Bornancin F, Renner F, Touil R, et al. Deficiency of MALT1 paracaspase activity results in unbalanced regulatory and effector T and B cell responses leading to multiorgan inflammation. *J Immunol*. 2015;194:3723–3734.
54. Gewies A, Gorka O, Bergmann H, et al. Uncoupling Malt1 threshold function from paracaspase activity results in destructive autoimmune inflammation. *Cell Rep*. 2014;9:1292–1305.
55. Demeyer A, Skordos I, Driege Y, et al. MALT1 proteolytic activity suppresses autoimmunity in a T cell intrinsic manner. *Front Immunol*. 2019;10:1898.
56. Demeyer A, Driege Y, Skordos I, et al. Long-term MALT1 inhibition in adult mice without severe systemic autoimmunity. *iScience*. 2020;23:101557.
57. Biswas S, Chalishazar A, Helou Y, et al. Pharmacological inhibition of MALT1 ameliorates autoimmune pathogenesis and can be uncoupled from effects on regulatory T-cells. *Front Immunol*. 2022;13:875320.
58. McGuire C, Elton L, Wieghofer P, et al. Pharmacological inhibition of MALT1 protease activity protects mice in a mouse model of multiple sclerosis. *J Neuroinflam*. 2014;11:124.
59. Kaufmann AM, Krise JP. Lysosomal sequestration of amine-containing drugs: analysis and therapeutic implications. *J Pharm Sci*. 2007;96:729–746.
60. Modica Napolitano JS, Aprille JR. Delocalized lipophilic cations selectively target the mitochondria of carcinoma cells. *Adv Drug Deliv Rev*. 2001;49:63–70.
61. Mempel TR, Krappmann D. Combining precision oncology and immunotherapy by targeting the MALT1 protease. *J Immunother Cancer*. 2022;10:e005442.
62. Gocher AM, Handu S, Workman CG. Interferon gamma production by regulatory T cells is required for response to cancer immunotherapy. *J Immunol*. 2020;204 (1Supp):244.8.